

# The analytical $\pi\pi$ scattering amplitude and the light scalars

N.N. Achasov<sup>a</sup> and A.V. Kiselev<sup>a,b</sup>

<sup>a</sup>*Laboratory of Theoretical Physics, Sobolev Institute*

*for Mathematics, 630090, Novosibirsk, Russia*

<sup>b</sup>*Novosibirsk State University, 630090, Novosibirsk, Russia*

(Dated: April 25, 2022)

## Abstract

In this work we construct the  $\pi\pi$  scattering amplitude  $T_0^0$  with regular analytical properties in the  $s$  complex plane, which describes simultaneously the data on the  $\pi\pi$  scattering,  $\phi \rightarrow \pi^0\pi^0\gamma$  decay, and  $\pi\pi \rightarrow K\bar{K}$  reaction. The chiral shielding of the  $\sigma(600)$  meson and its mixing with the  $f_0(980)$  meson are also taken into account. The data agrees with the four-quark nature of the  $\sigma(600)$  and  $f_0(980)$  mesons. The amplitude in the range  $-5m_\pi^2 < s < 0.64 \text{ GeV}^2$  also agrees with results, obtained on the base of the chiral expansion, dispersion relations, and the Roy equations.

PACS numbers: 12.39.-x 13.40.Hq 13.66.Bc

arXiv:1011.4446v2 [hep-ph] 16 Mar 2011

## I. INTRODUCTION

Study of light scalar resonances is one of the central problems of nonperturbative QCD, it is important for understanding both the confinement physics and the chiral symmetry realization way in the low energy region. The commonly suggested nonet of light scalar mesons is  $f_0(600)$  [or  $\sigma(600)$ ],  $K_0^*(800)$  [or  $\kappa(800)$ ],  $f_0(980)$ , and  $a_0(980)$  [1]. Light scalar mesons are intensively studied theoretically and experimentally in different reactions.

In Refs. [2] we described the high-statistical KLOE data on the  $\phi \rightarrow \pi^0\pi^0\gamma$  decay [3] simultaneously with the data on the  $\pi\pi$  scattering and the  $\pi\pi \rightarrow K\bar{K}$  reaction. The description was carried out taking into account the chiral shielding of the  $\sigma(600)$  meson [4, 5] and its mixing with the  $f_0(980)$  meson. It was shown that the data do not contradict the existence of the  $\sigma(600)$  meson and yield evidence in favor of the four-quark nature of the  $\sigma(600)$  and  $f_0(980)$  mesons.

This description revealed new goals. The point is that at the same time it was calculated in Ref. [6] the  $\pi\pi$  scattering amplitude in the  $s$  complex plane, basing on chiral expansion, dispersion relations, and Roy equations. In particular, the pole was obtained at  $s = M_\sigma^2 = (6.2 - 12.3i) m_\pi^2$ , where

$$M_\sigma = 441_{-8}^{+16} - i272_{-12.5}^{+9} \text{ MeV}, \quad (1)$$

which was assigned to the  $\sigma$  resonance.

Aiming the comparison of the results of Refs. [2] and [6] it is necessary to build the  $\pi\pi$  scattering amplitude with correct analytical properties in the complex  $s$  plane. The point is that in Ref. [2]  $S$  matrix of the  $\pi\pi$  scattering is the product of the "resonance" and "background" parts:

$$S_{\pi\pi} = S_{back} S_{res}, \quad (2)$$

and the  $S_{res}$  had correct analytical properties, while analytical properties of the  $S_{back}$  in the whole complex  $s$  plane were not essential for the aims of [2], where the physical region was investigated, and Adler zero existence [7] together with the poles absence on the real axis of the  $s$  complex plane were demanded.

In this paper we present the  $\pi\pi$  scattering amplitude with correct analytical properties in the complex  $s$  plane and the data description obtained with this amplitude [8]. The

comparison with the results of Ref. [6] is also presented.

All formulas for the  $\phi \rightarrow (S\gamma + \rho^0\pi^0) \rightarrow \pi^0\pi^0\gamma$  reaction [ $S = f_0(980) + \sigma(600)$ ] are shown in Sec. II. Our new parametrization of the background amplitude is presented in Secs. III and IV. The results of the data analysis are presented in Sec. V. A brief summary is given in Sec. VI.

## II. THEORETICAL DESCRIPTION OF THE $\phi \rightarrow (f_0(980) + \sigma(600))\gamma \rightarrow \gamma\pi^0\pi^0$ AND $\phi \rightarrow \rho^0\pi^0 \rightarrow \gamma\pi^0\pi^0$ REACTIONS

In Refs. [9, 10] it was shown that the dominant background process is  $\phi \rightarrow \pi^0\rho \rightarrow \gamma\pi^0\pi^0$ , while the reactions  $e^+e^- \rightarrow \rho \rightarrow \pi^0\omega \rightarrow \gamma\pi^0\pi^0$  and  $e^+e^- \rightarrow \omega \rightarrow \pi^0\rho \rightarrow \gamma\pi^0\pi^0$  have a small effect on  $e^+e^- \rightarrow \phi \rightarrow \gamma\pi^0\pi^0$  in the region  $m_{\pi^0\pi^0} \equiv m > 900$  MeV. In Ref. [11] it was shown that the  $\phi \rightarrow \pi^0\rho \rightarrow \gamma\pi^0\pi^0$  background is small in comparison with the signal  $\phi \rightarrow \gamma f_0(980) \rightarrow \gamma\pi^0\pi^0$  at  $m > 700$  MeV.

The amplitude of the background decay  $\phi(p) \rightarrow \pi^0\rho \rightarrow \gamma(q)\pi^0(k_1)\pi^0(k_2)$  has the following form:

$$M_{back} = F_b e^{-i\delta} g_{\rho\pi^0\phi} g_{\rho\pi^0\gamma} \phi_\alpha p_\nu \epsilon_\delta q_\epsilon \epsilon_{\alpha\beta\mu\nu} \epsilon_{\beta\delta\omega\epsilon} \left( \frac{k_{1\mu} k_{2\omega}}{D_\rho(q+k_2)} + \frac{k_{2\mu} k_{1\omega}}{D_\rho(q+k_1)} \right). \quad (3)$$

Here, constants  $F_b$  and  $\delta$  take into account  $\rho\pi$  rescattering effects [12]. Note that in this work and our previous work it was assumed that  $F_b = 1$  [13].

In the  $K^+K^-$  loop model,  $\phi \rightarrow K^+K^- \rightarrow \gamma(f_0 + \sigma)$  [9–11], above the  $K\bar{K}$  threshold the amplitude of the signal  $\phi \rightarrow \gamma(f_0 + \sigma) \rightarrow \gamma\pi^0\pi^0$  is

$$M_{sig} = g(m) \left( (\phi\epsilon) - \frac{(\phi q)(\epsilon p)}{(pq)} \right) T(K^+K^- \rightarrow \pi^0\pi^0) \times 16\pi, \quad (4)$$

where the  $K^+K^- \rightarrow \pi^0\pi^0$  amplitude, taking into account the mixing of  $f_0$  and  $\sigma$  mesons,

$$T(K^+K^- \rightarrow \pi^0\pi^0) = e^{i\delta_B} \sum_{R,R'} \frac{g_{RK^+K^-} G_{RR'}^{-1} g_{R'\pi^0\pi^0}}{16\pi}, \quad (5)$$

where  $R, R' = f_0, \sigma$ ,

$$\delta_B = \delta_B^{\pi\pi} + \delta_B^{K\bar{K}}, \quad (6)$$

where  $\delta_B^{\pi\pi}$  and  $\delta_B^{K\bar{K}}$  are phases of the elastic background of the  $\pi\pi$  and  $K\bar{K}$  scattering, respectively, see Refs. [14–17].

Note that the additional phase  $\delta_B^{K\bar{K}}$  changes the modulus of the  $K\bar{K} \rightarrow \pi^0\pi^0$  amplitude under the  $K\bar{K}$  threshold, at  $m < 2m_K$ . Let us define

$$P_K = \begin{cases} e^{i\delta_B^{K\bar{K}}} & m \geq 2m_K; \\ \text{analytical continuation of } e^{i\delta_B^{K\bar{K}}} & m < 2m_K. \end{cases} \quad (7)$$

Note also that the phase  $\delta_B^{\pi\pi}$  was defined as  $\delta_B$  in Refs. [10, 11].

The matrix of the inverse propagators [10] is

$$G_{RR'} \equiv G_{RR'}(m) = \begin{pmatrix} D_{f_0}(m) & -\Pi_{f_0\sigma}(m) \\ -\Pi_{f_0\sigma}(m) & D_\sigma(m) \end{pmatrix},$$

$$\Pi_{f_0\sigma}(m) = \sum_{a,b} \frac{g_{\sigma ab}}{g_{f_0 ab}} \Pi_{f_0}^{ab}(m) + C_{f_0\sigma},$$

where the constant  $C_{f_0\sigma}$  incorporates the subtraction constant for the transition  $f_0(980) \rightarrow (0^-0^-) \rightarrow \sigma(600)$  and effectively takes into account the contribution of multiparticle intermediate states to  $f_0 \leftrightarrow \sigma$  transition, see Ref. [10]. The inverse propagator of the R scalar meson is also presented in Refs. [9–11, 14–23]:

$$D_R(m) = m_R^2 - m^2 + \sum_{ab} [Re\Pi_R^{ab}(m_R^2) - \Pi_R^{ab}(m^2)], \quad (8)$$

where  $\sum_{ab} [Re\Pi_R^{ab}(m_R^2) - \Pi_R^{ab}(m^2)] = Re\Pi_R(m_R^2) - \Pi_R(m^2)$  takes into account the finite width corrections of the resonance which are the one loop contribution to the self-energy of the R resonance from the two-particle intermediate  $ab$  states.

For pseudoscalar  $a, b$  mesons and  $m_a \geq m_b$ ,  $m \geq m_+$  one has

$$\begin{aligned} \Pi_R^{ab}(m^2) = & \frac{g_{Rab}^2}{16\pi} \left[ \frac{m_+ m_-}{\pi m^2} \ln \frac{m_b}{m_a} + \right. \\ & \left. + \rho_{ab} \left( i + \frac{1}{\pi} \ln \frac{\sqrt{m^2 - m_-^2} - \sqrt{m^2 - m_+^2}}{\sqrt{m^2 - m_-^2} + \sqrt{m^2 - m_+^2}} \right) \right] \end{aligned} \quad (9)$$

$$m_- \leq m < m_+$$

$$\begin{aligned} \Pi_R^{ab}(m^2) = & \frac{g_{Rab}^2}{16\pi} \left[ \frac{m_+ m_-}{\pi m^2} \ln \frac{m_b}{m_a} - |\rho_{ab}(m)| + \right. \\ & \left. + \frac{2}{\pi} |\rho_{ab}(m)| \arctan \frac{\sqrt{m_+^2 - m^2}}{\sqrt{m^2 - m_-^2}} \right]. \end{aligned} \quad (10)$$

$m < m_-$

$$\begin{aligned} \Pi_R^{ab}(m^2) &= \frac{g_{Rab}^2}{16\pi} \left[ \frac{m_+ m_-}{\pi m^2} \ln \frac{m_b}{m_a} - \right. \\ &\quad \left. - \frac{1}{\pi} \rho_{ab}(m) \ln \frac{\sqrt{m_+^2 - m^2} - \sqrt{m_-^2 - m^2}}{\sqrt{m_+^2 - m^2} + \sqrt{m_-^2 - m^2}} \right]. \end{aligned} \quad (11)$$

$$\rho_{ab}(m) = \sqrt{\left(1 - \frac{m_+^2}{m^2}\right)\left(1 - \frac{m_-^2}{m^2}\right)}, \quad m_+ = m_a \pm m_b \quad (12)$$

The constants  $g_{Rab}$  are related to the width

$$\Gamma_R(m) = \sum_{ab} \Gamma(R \rightarrow ab, m) = \sum_{ab} \frac{g_{Rab}^2}{16\pi m} \rho_{ab}(m). \quad (13)$$

Note that we take into account intermediate states  $\pi\pi, K\bar{K}, \eta\eta, \eta'\eta, \eta'\eta'$  in the  $f_0(980)$  and  $\sigma(600)$  propagators:

$$\Pi_{f_0} = \Pi_{f_0}^{\pi^+\pi^-} + \Pi_{f_0}^{\pi^0\pi^0} + \Pi_{f_0}^{K^+K^-} + \Pi_{f_0}^{K^0\bar{K}^0} + \Pi_{f_0}^{\eta\eta} + \Pi_{f_0}^{\eta'\eta} + \Pi_{f_0}^{\eta'\eta'}, \quad (14)$$

and also for the  $\sigma(600)$ . We use  $g_{f_0 K^0 \bar{K}^0} = g_{f_0 K^+ K^-}$ ,  $g_{f_0 \pi^0 \pi^0} = g_{f_0 \pi^+ \pi^-} / \sqrt{2}$ , the same for the  $\sigma(600)$ , too.

For other coupling constants the naive four-quark model predicts [9, 21]

$$g_{f_0 \eta\eta} = -g_{f_0 \eta'\eta'} = \frac{2\sqrt{2}}{3} g_{f_0 K^+ K^-}, \quad g_{f_0 \eta'\eta} = -\frac{\sqrt{2}}{3} g_{f_0 K^+ K^-};$$

$$g_{\sigma\eta\eta} = g_{\sigma\eta'\eta'} = \frac{\sqrt{2}}{3} g_{\sigma\pi^+\pi^-}, \quad g_{\sigma\eta'\eta} = \frac{1}{3\sqrt{2}} g_{\sigma\pi^+\pi^-}.$$

The definition of  $g_{R\pi^0\pi^0}$ ,  $g_{R\eta\eta}$ ,  $g_{R\eta'\eta'}$  takes into account the identity of the particles. As these relations are approximate, we introduce the effective correction coefficients  $x_\sigma$  and  $x_{f_0}$ :

$$g_{f_0 \eta\eta} = -g_{f_0 \eta'\eta'} = \frac{2\sqrt{2}}{3} g_{f_0 K^+ K^-} x_{f_0}, \quad g_{f_0 \eta'\eta} = -\frac{\sqrt{2}}{3} g_{f_0 K^+ K^-} x_{f_0};$$

$$g_{\sigma\eta\eta} = g_{\sigma\eta'\eta'} = \frac{\sqrt{2}}{3} g_{\sigma\pi^+\pi^-} x_\sigma, \quad g_{\sigma\eta'\eta} = \frac{1}{3\sqrt{2}} g_{\sigma\pi^+\pi^-} x_\sigma.$$

In the  $K^+K^-$  loop model  $g(m)$  has the following forms (see Refs. [9, 20, 22, 23]).

For  $m < 2m_{K^+}$

$$\begin{aligned}
g(m) = & \frac{e}{2(2\pi)^2} g_{\phi K^+ K^-} \left\{ 1 + \frac{1 - \rho^2(m^2)}{\rho^2(m_\phi^2) - \rho^2(m^2)} \times \right. \\
& \left[ 2|\rho(m^2)| \arctan \frac{1}{|\rho(m^2)|} - \rho(m_\phi^2) \lambda(m_\phi^2) + i\pi \rho(m_\phi^2) - \right. \\
& \left. \left. - (1 - \rho^2(m_\phi^2)) \left( \frac{1}{4} (\pi + i\lambda(m_\phi^2))^2 - \right. \right. \right. \\
& \left. \left. \left. - \left( \arctan \frac{1}{|\rho(m^2)|} \right)^2 \right) \right] \right\}, \tag{15}
\end{aligned}$$

where

$$\rho(m^2) = \sqrt{1 - \frac{4m_{K^+}^2}{m^2}}; \quad \lambda(m^2) = \ln \frac{1 + \rho(m^2)}{1 - \rho(m^2)}; \quad \frac{e^2}{4\pi} = \alpha = \frac{1}{137}. \tag{16}$$

For  $m \geq 2m_{K^+}$

$$\begin{aligned}
g(m) = & \frac{e}{2(2\pi)^2} g_{\phi K^+ K^-} \left\{ 1 + \frac{1 - \rho^2(m^2)}{\rho^2(m_\phi^2) - \rho^2(m^2)} \times \right. \\
& \times \left[ \rho(m^2) (\lambda(m^2) - i\pi) - \rho(m_\phi^2) (\lambda(m_\phi^2) - i\pi) - \right. \\
& \left. \left. \frac{1}{4} (1 - \rho^2(m_\phi^2)) \left( (\pi + i\lambda(m_\phi^2))^2 - (\pi + i\lambda(m^2))^2 \right) \right] \right\}. \tag{17}
\end{aligned}$$

The mass spectrum of the reaction is

$$\frac{\Gamma(\phi \rightarrow \pi^0 \pi^0 \gamma)}{dm} = \frac{d\Gamma_S}{dm} + \frac{d\Gamma_{back}(m)}{dm} + \frac{d\Gamma_{int}(m)}{dm}, \tag{18}$$

where the signal contribution  $\phi \rightarrow S\gamma \rightarrow \pi^0 \pi^0 \gamma$

$$\frac{d\Gamma_S}{dm} = \frac{|P_K|^2 |g(m)|^2 \sqrt{m^2 - 4m_\pi^2} (m_\phi^2 - m^2)}{3(4\pi)^3 m_\phi^3} \left| \sum_{R,R'} g_{RK^+ K^-} G_{RR'}^{-1} g_{R' \pi^0 \pi^0} \right|^2. \tag{19}$$

The mass spectrum of the background process  $\phi \rightarrow \rho \pi^0 \rightarrow \pi^0 \pi^0 \gamma$

$$\frac{d\Gamma_{back}(m)}{dm} = \frac{1}{2} \frac{(m_\phi^2 - m^2) \sqrt{m^2 - 4m_\pi^2}}{256\pi^3 m_\phi^3} \int_{-1}^1 dx A_{back}(m, x), \tag{20}$$

where

$$A_{back}(m, x) = \frac{1}{3} \sum |M_{back}|^2 = \tag{21}$$

$$\begin{aligned}
&= \frac{F_b^2}{24} g_{\phi\rho\pi}^2 g_{\rho\pi\gamma}^2 \left\{ \left( m_\pi^8 + 2m^2 m_\pi^4 \tilde{m}_\rho^2 - 4m_\pi^6 \tilde{m}_\rho^2 + 2m^4 \tilde{m}_\rho^4 - \right. \right. \\
&\quad - 4m^2 m_\pi^2 \tilde{m}_\rho^4 + 6m_\pi^4 \tilde{m}_\rho^4 + 2m^2 \tilde{m}_\rho^6 - 4m_\pi^2 \tilde{m}_\rho^6 + \tilde{m}_\rho^8 - 2m_\pi^6 m_\phi^2 - \\
&\quad - 2m^2 m_\pi^2 \tilde{m}_\rho^2 m_\phi^2 + 2m_\pi^4 \tilde{m}_\rho^2 m_\phi^2 - 2m^2 \tilde{m}_\rho^4 m_\phi^2 + 2m_\pi^2 \tilde{m}_\rho^4 m_\phi^2 - 2\tilde{m}_\rho^6 m_\phi^2 + \\
&\quad + m_\pi^4 m_\phi^4 + \tilde{m}_\rho^4 m_\phi^4 \left. \right) \left( \frac{1}{|D_\rho(\tilde{m}_\rho)|^2} + \frac{1}{|D_\rho(\tilde{m}_\rho^*)|^2} \right) + (m_\phi^2 - m^2)(m^2 - \\
&\quad - 2m_\pi^2 + 2\tilde{m}_\rho^2 - m_\phi^2)(2m^2 m_\pi^2 + 2m_\pi^2 m_\phi^2 - m^4) \frac{1}{|D_\rho(\tilde{m}_\rho^*)|^2} + \\
&\quad + 2\text{Re} \left( \frac{1}{D_\rho(\tilde{m}_\rho) D_\rho^*(\tilde{m}_\rho^*)} \right) \left( m_\pi^8 - m^6 \tilde{m}_\rho^2 + 2m^4 m_\pi^2 \tilde{m}_\rho^2 + \right. \\
&\quad + 2m^2 m_\pi^4 \tilde{m}_\rho^2 - 4m_\pi^6 \tilde{m}_\rho^2 - 4m^2 m_\pi^2 \tilde{m}_\rho^4 + 6m_\pi^4 \tilde{m}_\rho^4 + \\
&\quad + 2m^2 \tilde{m}_\rho^6 - 4m_\pi^2 \tilde{m}_\rho^6 + \tilde{m}_\rho^8 + m^2 m_\pi^4 m_\phi^2 - 2m_\pi^6 m_\phi^2 + 2m^4 \tilde{m}_\rho^2 m_\phi^2 - \\
&\quad - 4m^2 m_\pi^2 \tilde{m}_\rho^2 m_\phi^2 + 2m_\pi^4 \tilde{m}_\rho^2 m_\phi^2 - m^2 \tilde{m}_\rho^4 m_\phi^2 + 2m_\pi^2 \tilde{m}_\rho^4 m_\phi^2 - 2\tilde{m}_\rho^6 m_\phi^2 - \\
&\quad \left. - m_\pi^4 m_\phi^4 - m^2 \tilde{m}_\rho^2 m_\phi^4 + 2m_\pi^2 \tilde{m}_\rho^2 m_\phi^4 + \tilde{m}_\rho^4 m_\phi^4 \right) \left. \right\},
\end{aligned}$$

$$\begin{aligned}
\tilde{m}_\rho^2 &= m_\pi^2 + \frac{(m_\phi^2 - m^2)}{2} (1 - x \sqrt{1 - \frac{4m_\pi^2}{m^2}}) \\
\tilde{m}_\rho^{*2} &= m_\phi^2 + 2m_\pi^2 - m^2 - \tilde{m}_\rho^2.
\end{aligned} \tag{22}$$

The interference between signal and background processes accounts for

$$\frac{d\Gamma_{int}(m)}{dm} = \frac{1}{\sqrt{2}} \frac{\sqrt{m^2 - 4m_\pi^2}}{256\pi^3 m_\phi^3} \int_{-1}^1 dx A_{int}(m, x), \tag{23}$$

where

$$\begin{aligned}
A_{int}(m, x) &= \frac{2}{3} (m_\phi^2 - m^2) \text{Re} \sum M_f M_{back}^* = \\
&= \frac{16\pi}{3} F_b \text{Re} \left\{ e^{i\delta} g(m) g_{\phi\rho\pi} g_{\rho\pi\gamma} T_0^0 (K^+ K^- \rightarrow \pi^0 \pi^0) \left[ \frac{(\tilde{m}_\rho^2 - m_\pi^2)^2 m_\phi^2 - (m_\phi^2 - m^2)^2 \tilde{m}_\rho^2}{D_\rho^*(\tilde{m}_\rho)} + \right. \right. \\
&\quad \left. \left. + \frac{(\tilde{m}_\rho^{*2} - m_\pi^2)^2 m_\phi^2 - (m_\phi^2 - m^2)^2 \tilde{m}_\rho^{*2}}{D_\rho^*(\tilde{m}_\rho^*)} \right] \right\} = \\
&= \frac{F_b}{3} \text{Re} \left\{ P_K e^{i\delta \frac{\pi}{B}} e^{i\delta} g(m) g_{\phi\rho\pi} g_{\rho\pi\gamma} \left( \sum_{R, R'} g_{RK^+ K^-} G_{RR'}^{-1} g_{R' \pi^0 \pi^0} \right) \times \right. \\
&\quad \left. \times \left[ \frac{(\tilde{m}_\rho^2 - m_\pi^2)^2 m_\phi^2 - (m_\phi^2 - m^2)^2 \tilde{m}_\rho^2}{D_\rho^*(\tilde{m}_\rho)} + \frac{(\tilde{m}_\rho^{*2} - m_\pi^2)^2 m_\phi^2 - (m_\phi^2 - m^2)^2 \tilde{m}_\rho^{*2}}{D_\rho^*(\tilde{m}_\rho^*)} \right] \right\}.
\end{aligned} \tag{24}$$

The factor 1/2 in Eq. (20) and the factor  $1/\sqrt{2}$  in Eq. (23) take into account the identity of pions.

The S-wave amplitude  $T_0^0$  of the  $\pi\pi$  scattering with I=0 [10, 15–17] is

$$T_0^0 = \frac{\eta_0^0 e^{2i\delta_0^0} - 1}{2i\rho_{\pi\pi}(m)} = \frac{e^{2i\delta_B^{\pi\pi}} - 1}{2i\rho_{\pi\pi}(m)} + e^{2i\delta_B^{\pi\pi}} \sum_{R,R'} \frac{g_{R\pi\pi} G_{RR'}^{-1} g_{R'\pi\pi}}{16\pi}. \quad (25)$$

Here  $\eta_0^0 \equiv \eta_0^0(m)$  is the inelasticity,  $\eta_0^0 = 1$  for  $m \leq 2m_{K^+}$ , and

$$\delta_0^0 \equiv \delta_0^0(m) = \delta_B^{\pi\pi}(m) + \delta_{res}(m), \quad (26)$$

where  $\delta_B^{\pi\pi} = \delta_B^{\pi\pi}(m)$  ( $\delta_B$  in Ref. [10]) is the phase of the elastic background [see Eq. 6], and  $\delta_{res}(m)$  is the resonance scattering phase,

$$S_0^{0\ res} = \eta_0^0(m) e^{2i\delta_{res}(m)} = 1 + 2i\rho_{\pi\pi}(m) \sum_{R,R'} \frac{g_{R\pi\pi} G_{RR'}^{-1} g_{R'\pi\pi}}{16\pi}, \quad \eta_0^0 = |S_0^{0\ res}|, \quad (27)$$

$g_{R\pi\pi} = \sqrt{3/2} g_{R\pi^+\pi^-}$ . The chiral shielding phase  $\delta_B^{\pi\pi}(m)$ , motivated by the  $\sigma$  model [4, 5] and desired analytical properties, is taken in more complicated form than in Ref. [2], see Sec. III.

The phase  $\delta_B^{K\bar{K}} = \delta_B^{K\bar{K}}(m)$  is parametrized in the following way:

$$\tan \delta_B^{K\bar{K}} = f_K(m^2) \sqrt{m^2 - 4m_{K^+}^2} \equiv 2p_K f_K(m^2) \quad (28)$$

and

$$e^{2i\delta_B^{K\bar{K}}} = \frac{1 + i2p_K f_K(m^2)}{1 - i2p_K f_K(m^2)} \quad (29)$$

Actually,  $e^{2i\delta_B^{\pi\pi}(m)}$  has a pole at  $m^2 = m_0^2$ ,  $0 < m_0^2 < 4m_\pi^2$ , which is compensated by the zero in  $e^{2i\delta_B^{K\bar{K}}(m)}$  to ensure a regular  $K\bar{K} \rightarrow \pi\pi$  amplitude and, consequently, the  $\phi \rightarrow K^+K^- \rightarrow \pi\pi\gamma$  amplitude at  $0 < m^2 < 4m_\pi^2$ . This requirement leads to

$$f_K(m_0^2) = \frac{1}{\sqrt{4m_{K^+}^2 - m_0^2}} \approx \frac{1}{2m_{K^+}}. \quad (30)$$

As in Refs. [2], for  $f_K(m^2)$  we used the form

$$f_K(m^2) = -\frac{\arctan\left(\frac{m^2 - m_1^2}{m_2^2}\right)}{\Lambda_K}. \quad (31)$$

The inverse propagator of the  $\rho$  meson has the following expression:

$$D_\rho(m) = m_\rho^2 - m^2 - im^2 \frac{g_{\rho\pi\pi}^2}{48\pi} \left(1 - \frac{4m_\pi^2}{m^2}\right)^{3/2}. \quad (32)$$

The coupling constants  $g_{\phi K^+ K^-} = 4.376 \pm 0.074$  and  $g_{\phi\rho\pi} = 0.814 \pm 0.018 \text{ GeV}^{-1}$  are taken from the most precise measurement [24]. To obtain the coupling constant  $g_{\rho\pi^0\gamma}$  we used the data of the experiments [25] and [26] on the  $\rho \rightarrow \pi^0\gamma$  decay and the expression

$$\Gamma(\rho \rightarrow \pi^0\gamma) = \frac{g_{\rho\pi^0\gamma}^2}{96\pi m_\rho^3} (m_\rho^2 - m_\pi^2)^3, \quad (33)$$

the result  $g_{\rho\pi^0\gamma} = 0.26 \pm 0.02 \text{ GeV}^{-1}$  is the weighed average of these experiments.

### III. THE BACKGROUND PHASE $\delta_B^{\pi\pi}$

The proper analytical properties of the  $\pi\pi$  scattering amplitude are two cuts in the  $s$ -complex plane, Adler zero in  $T_0^0$  [27], absence of poles on the physical sheet of the Riemannian surface,  $\sigma(600)$  and  $f_0(980)$  poles in the resonance amplitude on the second sheet of the Riemannian surface, and absence of poles on the second sheet in the background amplitude in the region  $4m_\pi^2 < \text{Re}(s) < (1.2 \text{ GeV})^2$ . This applies certain restrictions on the  $\delta_B^{\pi\pi}$ .

Let us represent  $\delta_B^{\pi\pi}$  in the physical region  $s = m^2 > 4m_\pi^2$  as

$$\tan(\delta_B^{\pi\pi}) = \frac{\text{Im}(P_{\pi 1}(s)P_{\pi 2}(s))}{\text{Re}(P_{\pi 1}(s)P_{\pi 2}(s))}, \quad (34)$$

and

$$e^{2i\delta_B^{\pi\pi}} = S_1^{\text{back}} S_2^{\text{back}} = \frac{P_{\pi 1}^*(s)P_{\pi 2}^*(s)}{P_{\pi 1}(s)P_{\pi 2}(s)} = \frac{P_{\pi 1}(s - i\epsilon)P_{\pi 2}(s - i\epsilon)}{P_{\pi 1}(s + i\epsilon)P_{\pi 2}(s + i\epsilon)}, \quad (35)$$

where

$$P_{\pi 1}(s) = a_1 - a_2 \frac{s}{4m_\pi^2} - \Pi_{\pi\pi}(s) + a_3 \Pi_{\pi\pi}(4m_\pi^2 - s) - a_4 Q_1(s), \quad (36)$$

$$Q_1(s) = \frac{1}{\pi} \int_{4m_\pi^2}^{\infty} \frac{s - 4m_\pi^2}{s' - 4m_\pi^2} \frac{\rho_{\pi\pi}(s')}{s' - s - i\epsilon} K_1(s'), \quad (37)$$

$$K_1(s) = \frac{L_1(s)}{D_1(4m_\pi^2 - s)D_2(4m_\pi^2 - s)D_3(4m_\pi^2 - s)D_4(4m_\pi^2 - s)D_5(4m_\pi^2 - s)D_6(4m_\pi^2 - s)}, \quad (38)$$

$$\begin{aligned}
L_1(s) = & (s - 4m_\pi^2)^6 + \alpha_1(s - 4m_\pi^2)^5 + \alpha_2(s - 4m_\pi^2)^4 + \alpha_3(s - 4m_\pi^2)^3 + \\
& + \alpha_4(s - 4m_\pi^2)^2 + \alpha_5(s - 4m_\pi^2) + \alpha_6 + \\
& + \sqrt{s} \left( c_1(s - 4m_\pi^2)^5 + c_2(s - 4m_\pi^2)^4 + c_3(s - 4m_\pi^2)^3 + \right. \\
& \left. + c_4(s - 4m_\pi^2)^2 + c_5(s - 4m_\pi^2) + c_6 \right), \tag{39}
\end{aligned}$$

$$D_i(s) = m_i^2 - s - g_i \Pi_{\pi\pi}(s), \tag{40}$$

$$\Pi_{\pi\pi}(s) = \frac{16\pi}{g_{Rab}^2} \Pi_R^{\pi\pi}(s), \tag{41}$$

$$P_{\pi 1}^*(s) = P_{\pi 1}(s - i\epsilon) = P_{\pi 1}(s) + 2i\rho_{\pi\pi}(s) \left( 1 + a_4 K_1(s) \right), \tag{42}$$

$$P_{\pi 2}(s) = \frac{\Lambda^2 + s - 4m_\pi^2}{4m_\pi^2} + k_2 Q_2(s), \tag{43}$$

here

$$Q_2(s) = \frac{1}{\pi} \int_{4m_\pi^2}^{\infty} \frac{s - 4m_\pi^2}{s' - 4m_\pi^2} \frac{\rho_{\pi\pi}(s')}{s' - s - i\epsilon} K_2(s'), \tag{44}$$

$$K_2(s) = \frac{L_2(s)}{D_{1A}(4m_\pi^2 - s) D_{2A}(4m_\pi^2 - s) D_{3A}(4m_\pi^2 - s)}, \tag{45}$$

$$L_2(s) = 4m_\pi^2 \left( s^2 + \beta s + \gamma_1 s^{3/2} + \gamma_2 s^{1/2} \right), \tag{46}$$

$$P_{\pi 2}^*(s) = P_{\pi 2}(s - i\epsilon) = P_{\pi 2}(s) - 2i\rho_{\pi\pi}(s) k_2 K_2(s). \tag{47}$$

Note that this parametrization was inspired by Ref. [19], devoted to proof that the propagators (8) satisfy the Källén-Lehmann representation in the wide domain of coupling constants of the scalar mesons with the two-particle states. Following the ideas of this paper the conditions

$$K_1(s) \geq 0, K_2(s) \geq 0 \text{ at } s > 4m_\pi^2$$

guarantee absence of poles on the physical sheet in Eq. (35) (of course, the restrictions of Sec. IV should be fulfilled too). Note also that we choose the denominator of (35) as  $P_{\pi_1}(s)P_{\pi_2}(s)$  for our comfort.

#### IV. RESTRICTIONS ON THE PARAMETERS

Some parameters are fixed by the requirement of the proper analytical continuation of amplitudes. The denominators  $P_{\pi_1}$  and  $P_{\pi_2}$  have zeroes at  $s = m_0^2$  and  $s = m_{0A}^2$  respectively, both belonging to the interval  $0 < s < 4m_\pi^2$ . These zeroes should be compensated by zeroes in any pair from  $P_{\pi_1}^*$ ,  $P_{\pi_2}^*$  and  $S_0^{0\ res}$ . We choose

$$\begin{aligned} P_{\pi_1}^*(m_0^2) &= 0, \\ S_0^{0\ res}(m_{0A}^2) &= 0, \end{aligned} \tag{48}$$

see Eq. (35) [28].

The requirement of the  $T_0^0$  finiteness at  $s = 0$  leads to 2 conditions. Really, on the real axis for  $s > 4m_\pi^2$  we have

$$\begin{aligned} S_1^{back} &= \frac{P_{\pi_1}^*(s)}{P_{\pi_1}(s)} = \frac{P_{\pi_1}(s - i\epsilon)}{P_{\pi_1}(s + i\epsilon)} = 1 + 2i\rho_{\pi\pi}(s) \frac{1 + K_1(s)}{P_{\pi_1}(s)}, \\ S_2^{back} &= \frac{P_{\pi_2}^*(s)}{P_{\pi_2}(s)} = \frac{P_{\pi_2}(s - i\epsilon)}{P_{\pi_2}(s + i\epsilon)} = 1 - 2i\rho_{\pi\pi}(s) \frac{K_2(s)}{P_{\pi_2}(s)}. \end{aligned}$$

So, to avoid singularity in the

$$T_0^0 = \frac{S_1^{back} S_2^{back} S_0^{0\ res} - 1}{2i\rho_{\pi\pi}(s)}$$

at  $s = 0$ , where  $\rho_{\pi\pi}(s)$  becomes infinite, we require

$$1 + K_1(0) = 0,$$

as for  $K_2(0)$ , it is equal to zero at  $s = 0$  via construction, see Eq. (45). Note that, alternatively, one may require  $T_0^{0\ res}(0) = 0$ .

Additionally, as it was noted in Refs. [29], crossing symmetry implemented by Roy equations imposes the condition

$$\frac{dT_0^0}{dm}(m^2 = 0) = 0.$$

Recall that the condition Eq. (30) removes the singularity in the  $T(\pi\pi \rightarrow K\bar{K})$  amplitude. One can see that no special prerequisite to Adler zero existence in the  $\pi\pi$  scattering amplitude should be imposed, because it appears when we take into account the results of Ref. [6].

## V. DATA ANALYSIS

Analyzing data, we imply a scenario motivated by the four-quark model [30], that is, the  $\sigma(600)$  coupling with the  $K\bar{K}$  channel,  $g_{\sigma K^+K^-}$ , is suppressed relatively to the coupling with the  $\pi\pi$  channel,  $g_{\sigma\pi^+\pi^-}$ , the mass of the  $\sigma$  meson  $m_\sigma$  is in the 500-700 MeV range. In addition, we have in mind the Adler self-consistency conditions for the  $T_0^0(\pi\pi \rightarrow \pi\pi)$  near the  $\pi\pi$  threshold. The general aim of this section is to demonstrate that the data and the [6] results on the  $\pi\pi$  amplitude are in excellent agreement with this general scenario.

As in Ref. [2] for  $\phi \rightarrow \pi^0\pi^0\gamma$  decay we use the KLOE data [3] for  $m > 660$  MeV. For the  $\delta_0^0$  we use the "old data" [31–35], 44 points up to 1.2 GeV [36]. Besides, we take into account the new precise data in the low energy region [37, 38].

The inelasticity  $\eta_0^0(m)$  and the phase  $\delta^{\pi K}(m)$  of the amplitude  $T(\pi\pi \rightarrow K\bar{K})$  are essential in the fit region,  $2m_{K^+} < m < 1.2$  GeV. As for the inelasticity, the experimental data of Ref. [31] gives evidence in favor of low values of  $\eta_0^0(m)$  near the  $K\bar{K}$  threshold. At present the contribution of the  $\eta\eta$ ,  $\eta'\eta$ , and  $\eta'\eta'$  channels does not affect much the overall fits. To fix a relation between the  $K\bar{K}$  and  $\eta\eta$  channels reliably the inelasticity should be measured with accuracy 10 times better than the existing one. The situation with the experimental data on  $\delta^{\pi K}(m)$  is controversial and experiments have large errors. We consider these data as a guide, whose main role is to fix the sign between signal (4) and background amplitudes (3), and hold two points of the experiment [39], see Fig. 9. As for inelasticity, for fitting we used only the key experimental point  $\eta_0^0(m = 1.01 \text{ GeV}) = 0.41 \pm 0.14$ , see Fig. 5.

Providing all the above conditions, we have obtained perfect agreement with the general scenario under consideration, see Fits 1, 2 in Tables I, II, and III and Figs. 1-10. Fits 1 and 2 show that the allowed range of  $\sigma(600)$  and  $f_0(980)$  parameters is rather wide.

The values of  $g_{f_0 K^+K^-}^2/4\pi$  in Fits 1 and 2 (1 GeV<sup>2</sup> and 2 GeV<sup>2</sup>, correspondingly) show a

scale of possible deviation of this constant. This may be important to coordinate  $g_{f_0 K^+ K^-}^2/4\pi$  with  $g_{a_0 K^+ K^-}^2/4\pi$  [40], note the latter is usually larger than 1 GeV<sup>2</sup>.

In addition, we carry out Fit 3, where  $\sigma(600)$  and  $f_0(980)$  are coupled only with the  $\pi\pi$  channel. As seen from Table I and Figs. 11-13, Fit 3 is in excellent agreement with the data on the  $\delta_0^0$  up to 1 GeV and the [6] results.

We introduce 52 parameters, but for restrictions (expresses 5 parameters through others) and parameters (or their combinations), that go to the bound of the permitted range (7 effective links), the effective number of free parameters is reduced to 40. It is significant that fits describe not only the experimental data (about 80 points), but also the  $\pi\pi$  amplitude from the [6] in the range  $-5m_\pi^2 < s < 0.64$  GeV<sup>2</sup> which is treated along with experimental data.

The  $\sigma(600)$  pole positions, obtained in Fits 1 and 2, lie far from Eq. (1), see Table I. One of the possible reasons is neglecting  $K\bar{K}$  and other high channels in the [6] approach. The role of high channels can be estimated with the help of Fit 3, whose  $\sigma(600)$  pole position is considerably closer to Eq. (1), see Table I.

Note that kernels of the background integrals (38) and (45) are positive in the range of integration  $[2m_\pi, \infty)$ , Fit 1 kernels are presented in Fig. 7.

The Adler zero in the  $T_0^0(\pi\pi \rightarrow \pi\pi)$  is near  $s = (100 \text{ MeV})^2$  in all Fits because we describe the amplitude [6]. Fit 2 also has Adler zero in the  $T(\pi\pi \rightarrow K\bar{K})$  at  $s = (166 \text{ MeV})^2$ , Fit 1 has a zero in the  $T(\pi\pi \rightarrow K\bar{K})$  at  $s = -(601 \text{ MeV})^2$ .

The resonance amplitude  $T_0^{0res}$  has poles on the unphysical sheets of its Riemannian surface. As we have a multichannel case, the amplitude has the set of lists depending on lists of the polarization operators  $\Pi_R^{ab}(s)$ . We show resonance poles only on some lists, see Tables IV and V. For this choice, in case of metastable states, decaying to several channels, the imaginary parts of pole positions  $M_R$  would be connected to the full widths of the resonances  $[2\text{Im}M_R = \Gamma_R = \sum_{ab} \Gamma(R \rightarrow ab)]$ . Note that  $\sigma(600)$  and  $f_0(980)$  poles, shown in Table I, correspond to the first lines of Tables IV and V.

As to the background amplitude  $T_0^{0back}$ , it has poles on the second sheet of the Riemannian surface, where  $P_{\pi 1} = 0$  or  $P_{\pi 2} = 0$ . The  $P_{\pi 1}$  has a zero at  $s = (1246 - 104i)^2 \text{ MeV}^2$  for Fit 1, at  $s = (1354 - 110i)^2 \text{ MeV}^2$  for Fit 2, and at  $s = (1056 - 142i)^2 \text{ MeV}^2$  for Fit 3. The  $P_{\pi 2}$  has a zero at  $s = (0.2 - 9.5i) m_\pi^2$  for Fit 1, at  $s = (2.0 - 8.9i) m_\pi^2$  for Fit 2, and at  $s = (-0.6 - 8.6i) m_\pi^2$  for Fit 3. These poles lie outside of the region  $4m_\pi^2 < \text{Re}(s) < (1.2$

$\text{GeV}^2$  except the pole at  $s = (1056 - 142i)^2 \text{ MeV}^2$  for Fit 3, but for this Fit the upper bound is  $1 \text{ GeV}^2$ .

Table I. Properties of the resonances and main characteristics are shown.

Fit	1	2	3
$m_{f_0}$ , MeV	979.16	986.50	964.01
$g_{f_0 K^+ K^-}$ , GeV	3.54	5.01	0
$\frac{g_{f_0 K^+ K^-}^2}{4\pi}$ , $\text{GeV}^2$	1	2	0
$g_{f_0 \pi^+ \pi^-}$ , GeV	-1.3737	-2.1185	0.3183
$\frac{g_{f_0 \pi^+ \pi^-}^2}{4\pi}$ , $\text{GeV}^2$	0.150	0.357	0.008
$x_{f_0}$	0.6640	0.9584	-
$\Gamma_{f_0}(m_{f_0})$ , MeV	55.2	130.3	3.0
$f_0(980)$ pole, MeV	$986.2 - 25.5i$	$990.5 - 19.4i$	$978.9 - 11.4i$
$m_\sigma$ , MeV	487.59	506.95	480.46
$g_{\sigma \pi^+ \pi^-}$ , GeV	2.7368	2.6735	2.5871
$\frac{g_{\sigma \pi^+ \pi^-}^2}{4\pi}$ , $\text{GeV}^2$	0.596	0.569	0.533
$g_{\sigma K^+ K^-}$ , GeV	0.552	0.774	0
$\frac{g_{\sigma K^+ K^-}^2}{4\pi}$ , $\text{GeV}^2$	0.024	0.048	0
$x_\sigma$	0.9750	0.8201	0
$\Gamma_\sigma(m_\sigma)$ , MeV	377.8	352.9	340.2
$\sigma(600)$ pole, MeV	$581.0 - 212.7i$	$613.8 - 221.4i$	$528.6 - 220.3i$
$C$ , $\text{GeV}^2$	0.04317	-0.07633	-0.11734
$\delta$ , $^\circ$	-70.62	-73.6	-
$m_1$ , MeV	801.90	814.88	-
$m_2$ , MeV	465.95	554.95	-
$\Lambda_K$ , GeV	1.142	1.030	-
$a_0^0$ , $m_\pi^{-1}$	0.223	0.226	0.221
Adler zero in $\pi\pi \rightarrow \pi\pi$	$(94.4 \text{ MeV})^2$	$(96.8 \text{ MeV})^2$	$(87.1 \text{ MeV})^2$
$\eta_0^0(1010 \text{ MeV})$	0.55	0.45	-
$\chi_{phase}^2$ (44 points)	45.9	50.6	26.3 (34 points)
$\chi_{sp}^2$ (18 points)	24.9	19.1	-

Table II. Parameters of the first background ( $P_{\pi 1}$ ) are shown.

Fit	1	2	3
$a_1$	-3.105	-4.549	-1.498
$a_2$	0.01136	0.00998	0.05821
$a_3$	0	0	0
$a_4$	4.9328	13.1111	1.2475
$\alpha_1, \text{GeV}^2$	604.137	624.512	-792.804
$\alpha_2, \text{GeV}^4$	920.111	1000.739	-384.477
$\alpha_3, \text{GeV}^6$	785.958	781.770	416.645
$\alpha_4, \text{GeV}^8$	223.623	211.195	198.772
$\alpha_5, \text{GeV}^{10}$	24.5339	23.8517	25.4265
$\alpha_6, \text{GeV}^{12}$	0.248657	0.314094	0.198560
$c_1, \text{GeV}$	356.128	224.404	995.905
$c_2, \text{GeV}^3$	-2735.40	-2600.82	-1070.75
$c_3, \text{GeV}^5$	284.008	445.192	542.745
$c_4, \text{GeV}^7$	430.758	461.717	411.927
$c_5, \text{GeV}^9$	49.7913	47.2357	51.4206
$c_6, \text{GeV}^{11}$	-0.664290	-0.684002	-0.635647
$m_1, \text{MeV}$	1105.67	1111.87	1002.31
$g_1, \text{MeV}$	347.70	350.48	306.18
$m_2, \text{MeV}$	1061.53	1141.92	806.93
$g_2, \text{MeV}$	344.12	381.73	350.51
$m_3, \text{MeV}$	1061.85	1169.51	781.76
$g_3, \text{MeV}$	311.56	311.80	322.57
$m_4, \text{MeV}$	970.78	1040.96	970.78
$g_4, \text{MeV}$	457.52	455.56	376.88
$m_5, \text{MeV}$	1176.39	1320.55	1153.21
$g_5, \text{MeV}$	544.43	588.48	500.59
$m_6, \text{MeV}$	1521.20	1621.10	1808.74
$g_6, \text{MeV}$	739.93	750.75	841.57

Table III. Parameters of the second background ( $P_{\pi_2}$ ) are shown.

Fit	1	2	3
$\Lambda$ , MeV	83.238	74.477	70.268
$k_2$	0.0152934	0.0168176	0.0150655
$\beta$	239.184	221.055	263.511
$\gamma_1$	1006.367	928.743	878.056
$\gamma_2$	22.7004	23.3341	29.4097
$m_{1A}$ , MeV	491.92	84.77	687.43
$g_{1A}$ , MeV	469.29	492.03	364.68
$m_{2A}$ , MeV	531.81	639.95	528.40
$g_{2A}$ , MeV	452.20	261.48	378.65
$m_{3A}$ , MeV	670.64	565.16	608.72
$g_{3A}$ , MeV	299.23	428.97	370.98

Table IV.  $\sigma(600)$  poles (MeV) on different sheets of the complex  $s$  plane depending on lists of polarization operators  $\Pi^{ab}(s)$  are shown.

$\Pi^{K\bar{K}}$ list	$\Pi^{\eta\eta}$ list	$\Pi^{\eta\eta'}$ list	$\Pi^{\eta'\eta'}$ list	Fit 1	Fit 2
I	I	I	I	$581.0 - 212.7i$	$613.8 - 221.4i$
II	I	I	I	$617.5 - 353.0i$	$609.8 - 291.6i$
II	II	I	I	$554.3 - 375.3i$	$559.4 - 346.6i$
II	II	II	I	$579.0 - 475.2i$	$569.7 - 410.7i$
II	II	II	II	$625.7 - 474.9i$	$581.6 - 411.0i$

Table V.  $f_0(980)$  poles (MeV) on different sheets of the complex  $s$  plane depending on lists of polarization operators  $\Pi^{ab}(s)$  are shown.

$\Pi^{K\bar{K}}$ list	$\Pi^{\eta\eta}$ list	$\Pi^{\eta\eta'}$ list	$\Pi^{\eta'\eta'}$ list	Fit 1	Fit 2
I	I	I	I	$986.2 - 25.5i$	$990.5 - 19.4i$
II	I	I	I	$916.9 - 299.4i$	$1183.2 - 518.6i$
II	II	I	I	$966.8 - 450.5i$	$1366.0 - 756.5i$
II	II	II	I	$962.6 - 465.2i$	$1390.7 - 813.0i$
II	II	II	II	$962.5 - 608.0i$	$1495.6 - 1057.7i$

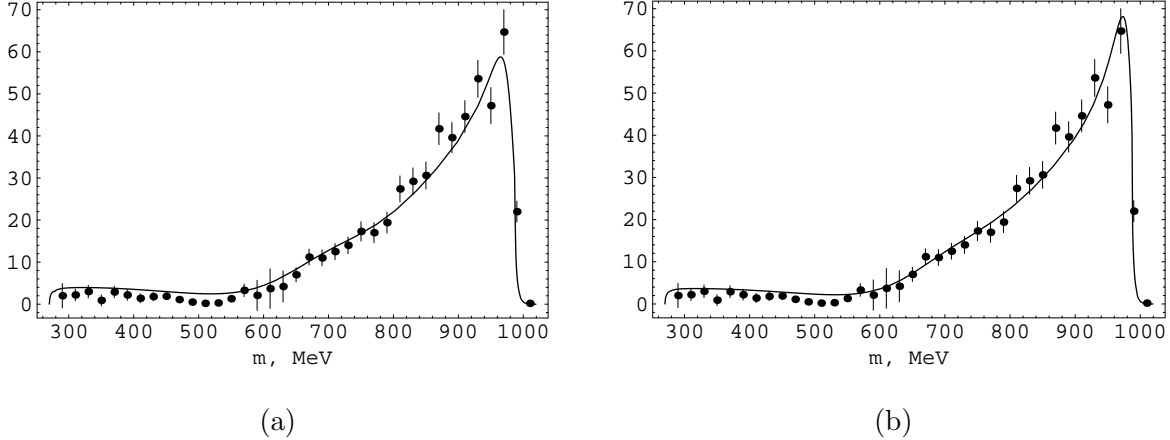


FIG. 1: The  $\pi^0\pi^0$  spectrum in the  $\phi \rightarrow \pi^0\pi^0\gamma$  decay, theoretical curve, and the KLOE data (points) are shown: a) Fit 1, b) Fit 2.

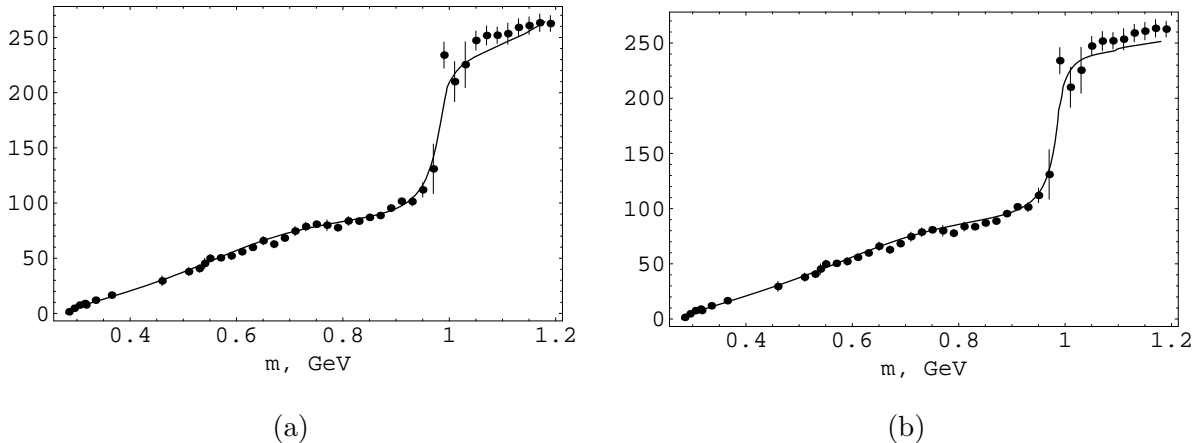


FIG. 2: The phase  $\delta_0^0$  of the  $\pi\pi$  scattering (degrees) is shown: a) Fit 1, b) Fit 2.

Note it would be naive to treat the poles in the background as resonances [ $f_0(1370)$ , for example] because in our approach to consider additional resonances one should extend the matrix of the inverse propagators, etc.

## VI. CONCLUSION

Thus, the background phase (34) allows us to obtain proper analytical features of the  $\pi\pi$  scattering amplitude, link results of [6] with properties of light scalars simultaneously describing experimental data. The obtained description is in agreement with the scenario based on the four-quark model. The main signatures of this scenario are the weak coupling

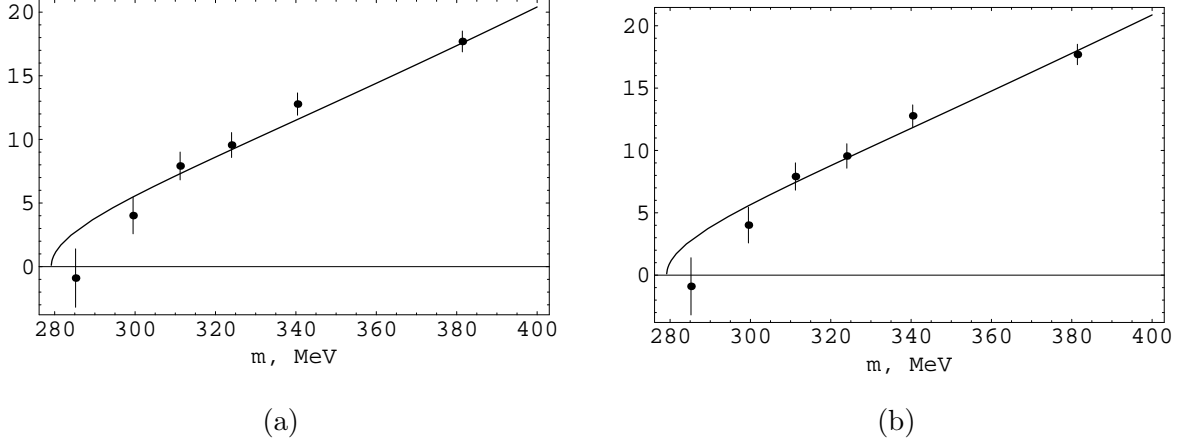


FIG. 3: The comparison of the experimental data on  $\delta_0^0$  [37] and the obtained curve is shown: a) Fit 1, b) Fit 2.

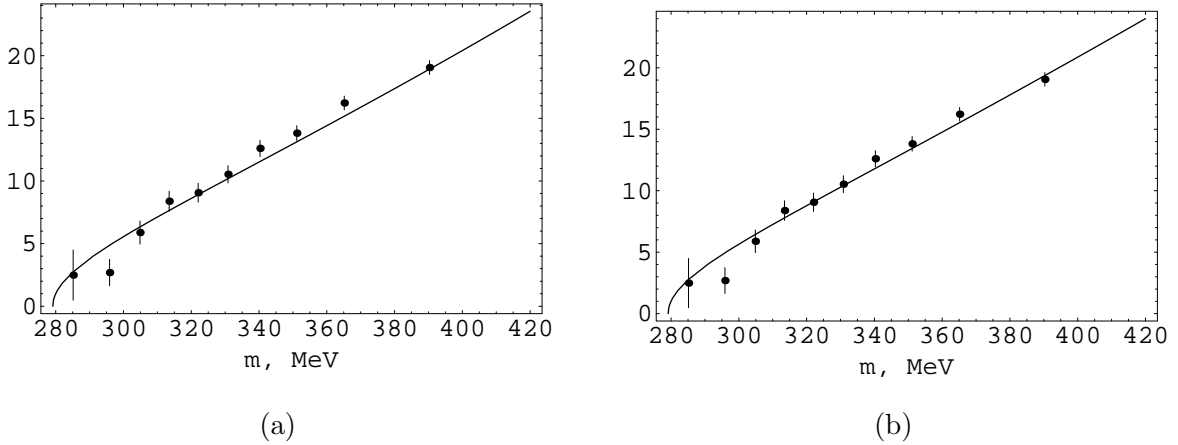


FIG. 4: The comparison of the experimental data on  $\delta_0^0$  [38] and the obtained curve is shown: a) Fit 1, b) Fit 2.

of the  $\sigma(600)$  meson with the  $K\bar{K}$  channel compared to the  $\pi\pi$  one and the weak coupling of the  $f_0(980)$  meson with the  $\pi\pi$  channel compared to the  $K\bar{K}$  one, see Table I, that results in the weak  $\sigma(600) - f_0(980)$  mixing [2]. The ratios  $(g_{\sigma K^+K^-}/g_{\sigma\pi^+\pi^-})^2 \approx 0.05 - 0.1$  and  $(g_{f_0\pi^+\pi^-}/g_{f_0K^+K^-})^2 \approx 0.15 - 0.18$ , see Table I, indicate roughly that the 90 percentage of  $\sigma(600)$  is  $\bar{u}dud$  and the 80 percentage of  $f_0(980)$  is  $\bar{s}dds$ .

Resonance masses and widths  $m_R$  and  $\Gamma_R(m_R)$  in our formulas (which may be called "Breit-Wigner" masses and widths) have clear physical meaning, in contrast to the resonance poles in the complex plane. At first, what sheet of the complex plane should be considered?

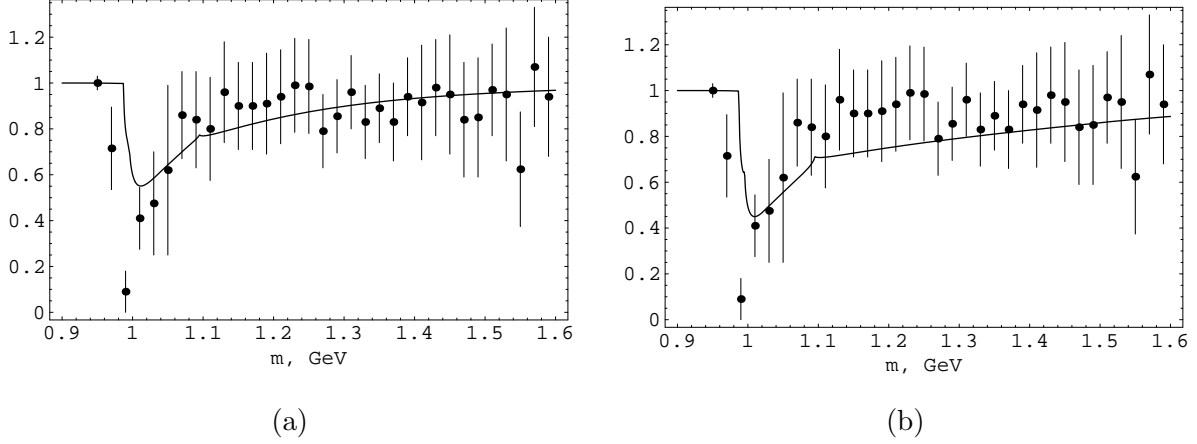


FIG. 5: The inelasticity  $\eta_0^0$  is shown: a) Fit 1, b) Fit 2.

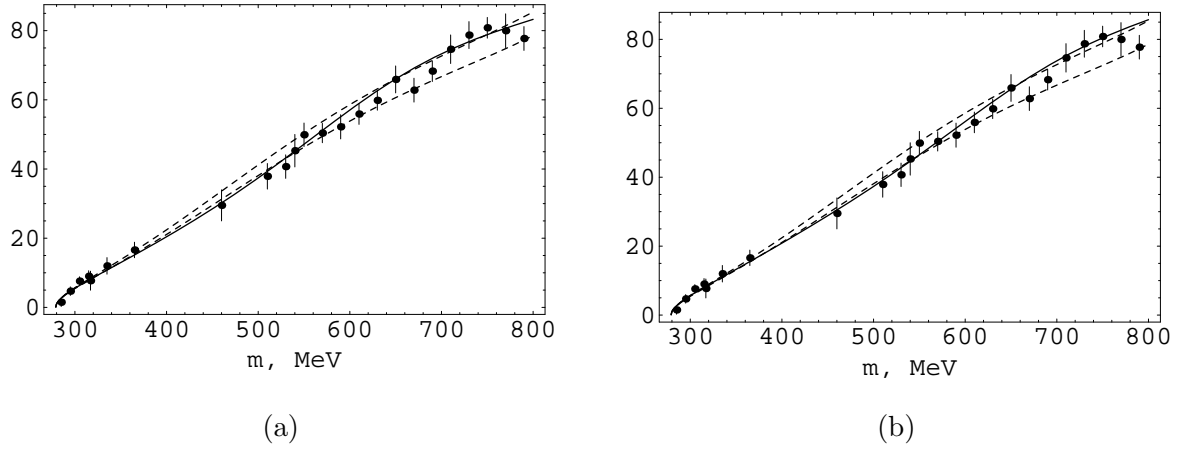


FIG. 6: The phase  $\delta_0^0$  of the  $\pi\pi$  scattering is shown. The solid line is our description, dashed lines mark borders of the corridor [6], and points are experimental data: a) Fit 1, b) Fit 2.

For  $\sigma(600)$  it is natural to consider the first line of Table IV [at any rate, it would be correct for very narrow  $\sigma(600)$ ]. The obtained pole positions in this case do not agree with the pole position obtained in Ref. [6], see Eq. (1). Note that the  $\sigma(600)$  pole position is dictated by the  $\sigma(600)$  propagator in our case, because the  $\sigma(600) - f_0(980)$  mixing is small. Providing the pole position (1) and taking into account only the  $\pi\pi$  channel in the propagator, we can determine  $\sigma(600)$  mass and coupling to the  $\pi\pi$  channel, and the obtained values contradict the Källén-Lehmann representation, see [19]. Taking into account additional channels we may fulfill the Källén-Lehmann representation, but the region of permitted  $\sigma(600)$  parameters do not allow us to describe experimental data in the current

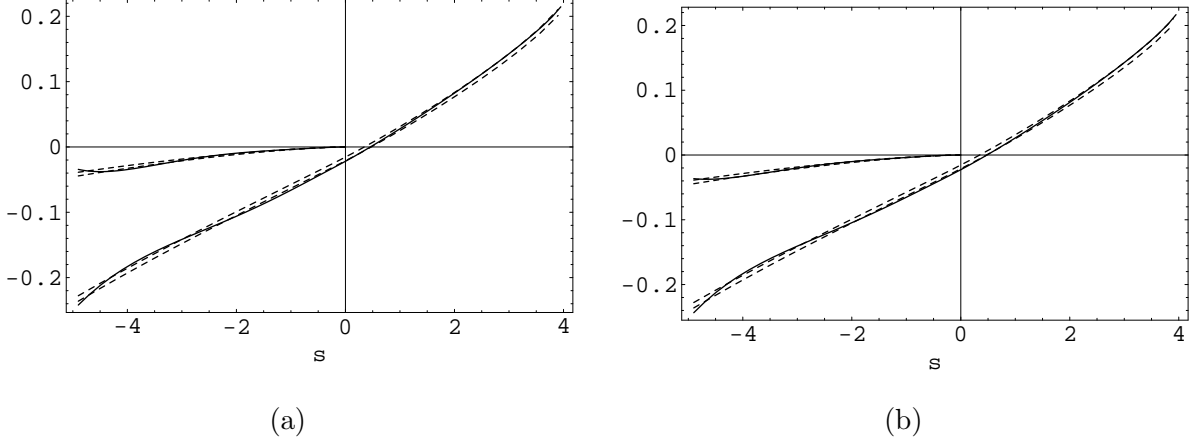


FIG. 7: The real and the imaginary parts of the amplitude  $T_0^0$  of the  $\pi\pi$  scattering ( $s$  in units of  $m_\pi^2$ ) are shown. Solid lines show our description, dashed lines mark borders of the real part corridor and the imaginary part for  $s < 0$  [6]: a) Fit 1; b) Fit 2.

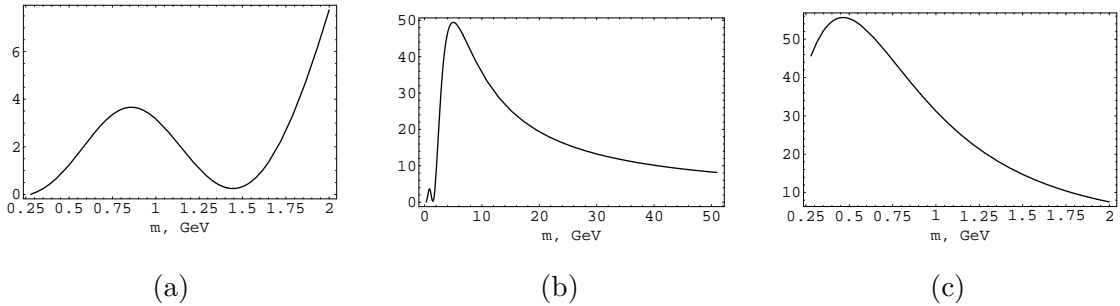


FIG. 8: Kernels  $K_1(m^2)$  and  $K_2(m^2)$  for Fit 1 are shown: a)  $K_1(m^2)$  below 2 GeV. The minimum near 1.4 GeV is 0.25. b)  $K_1(m^2)$  up to 50 GeV, then it asymptotically tends to 1. c)  $K_2(m^2)$  up to 2 GeV, then it asymptotically tends to zero.

model.

Note that the Roy equations are approximate, they take into account only the  $\pi\pi$  channel. This can lead to a different analytical continuation and, hence, explain deviation of the  $\sigma(600)$  pole position, compare Fit 3 with Fits 1 and 2 in Table I [41].

The current activity, aiming extremely precise determination of the  $\sigma(600)$  pole position, has taken the forms of the Swift's grotesque. Really, the residue of the  $\sigma$  pole can not be connected to coupling constant in the Hermitian (or quasi-Hermitian) Hamiltonian, see Ref. [5], for it has a large imaginary part and this pole can not be interpreted as a physical state for its huge width.

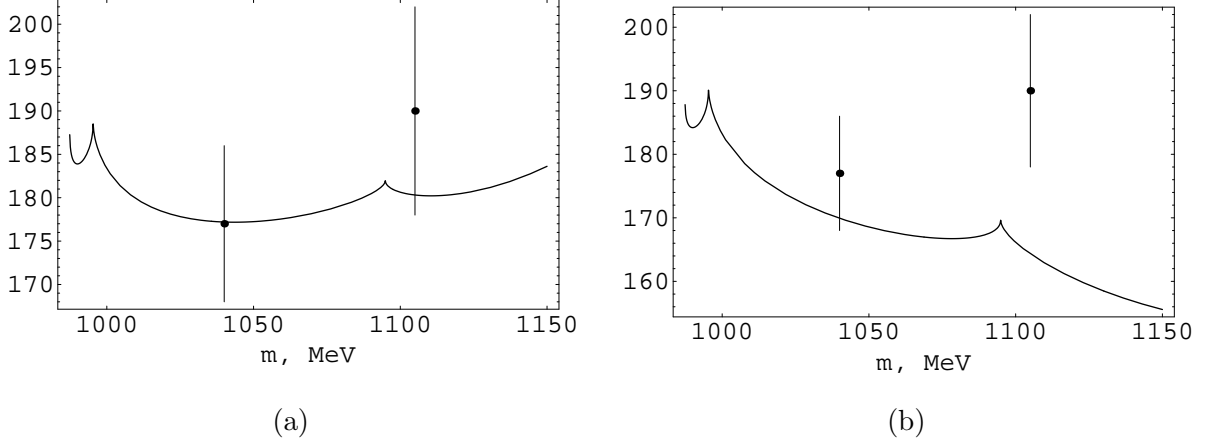


FIG. 9: The phase  $\delta^{\pi K}$  of the  $\pi\pi \rightarrow K\bar{K}$  scattering is shown: a) Fit 1; b) Fit 2.

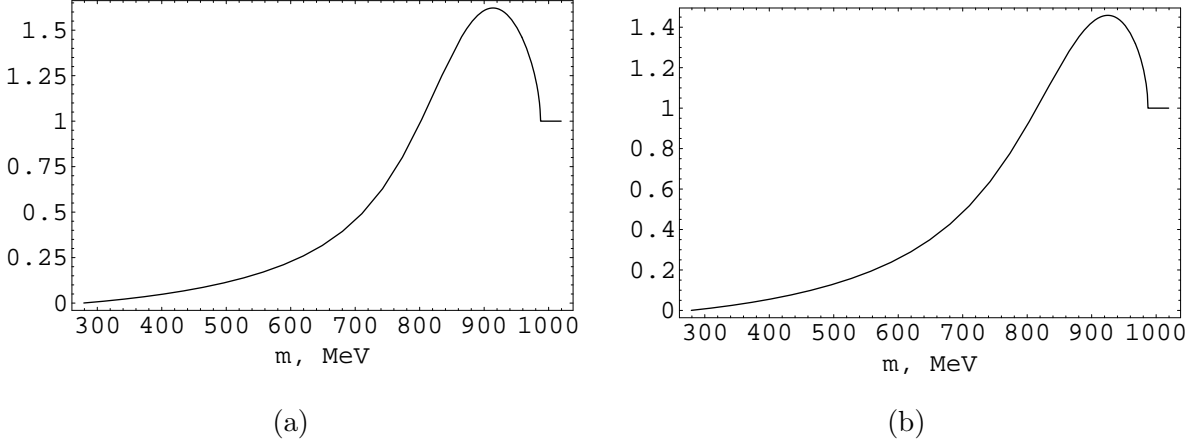


FIG. 10: The  $|P_K(m)|^2$  is shown, see Eq. (7): a) Fit 1; b) Fit 2.

The futility of the approach that is based on the poles treatment may be additionally illustrated by Fit 2. As seen on line 1 of Table V, the real part of the  $f_0(980)$  pole  $ReM_{f_0}$  on the II sheet of the  $T_0^0$  exceeds the  $K^+K^-$  threshold (987.4 MeV), it means that  $ImM_{f_0}$  equals to  $-\left(\Gamma(f_0(980) \rightarrow \pi\pi) - \Gamma(f_0(980) \rightarrow K^+K^-)\right)/2$ , which is physically meaningless. In this case we should take  $\Pi^{K^+K^-}$  from the second sheet, this gives the pole at  $M_{f_0} = 989.6 - 168.7 i$  MeV, with  $ReM_{f_0}$  between the  $K^+K^-$  and  $K^0\bar{K}^0$  thresholds again. As we work on the  $s$  plane, we should consider not  $M_{f_0}$ , but  $M_{f_0}^2 = (0.951 - 0.334 i)$  GeV<sup>2</sup>. So, we have the pole with a real part below the  $K^+K^-$  and  $K^0\bar{K}^0$  thresholds and an imaginary part dictated by analytical continuation of the kaon polarization operators.

To reduce an effect of heavier isosinglet scalars we restrict ourselves to the analysis of the

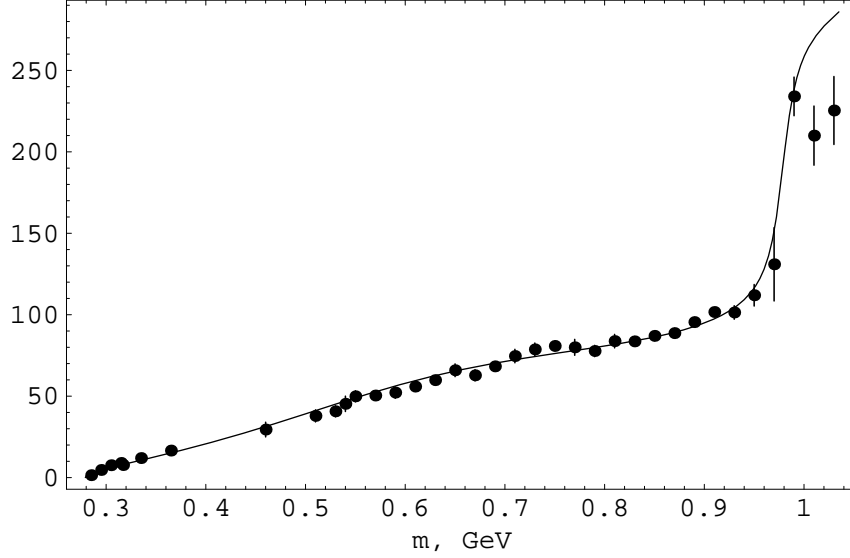


FIG. 11: The phase  $\delta_0^0$  of the  $\pi\pi$  scattering, Fit 3 and the experimental data are shown.

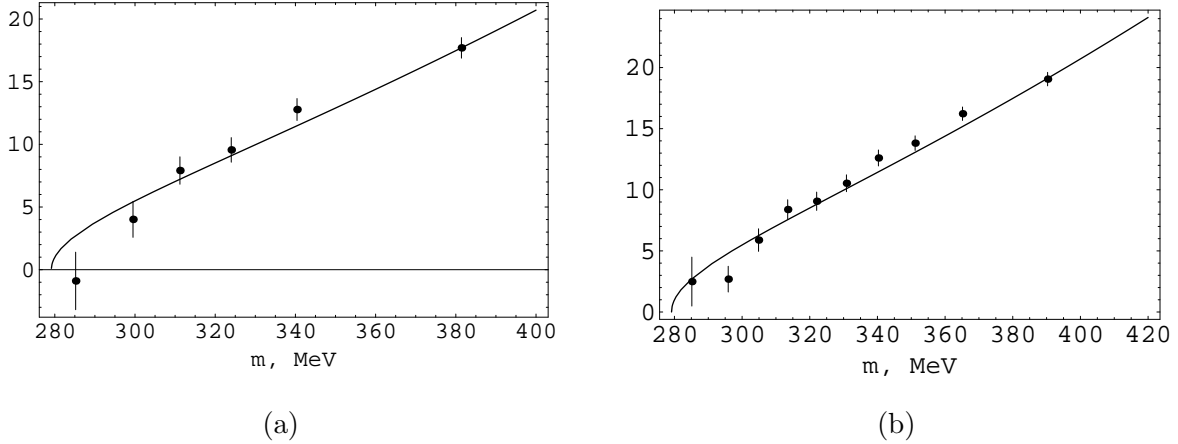


FIG. 12: The phase  $\delta_0^0$  of the  $\pi\pi$  scattering, Fit 3 is shown. The comparison with the data is available from a) [37], b) [38].

mass region  $m < 1.2$  GeV. As to mixing light and heavier isosinglet scalars, this question could not be resolved once and for all at present, in particular, because their properties are not well established up to now. A preliminary consideration was carried out in Ref. [42], where, in particular, it was shown that the mixing could affect the mass difference of the isoscalar and isovector.

The factor  $|P_K(s)|^2$  modifying the  $|T(\pi\pi \rightarrow K\bar{K})|^2$ , see Eqs. (7) and (31), is shown on Fig. 10. This factor does not change the kaon loop model radically, but helps to fulfill the

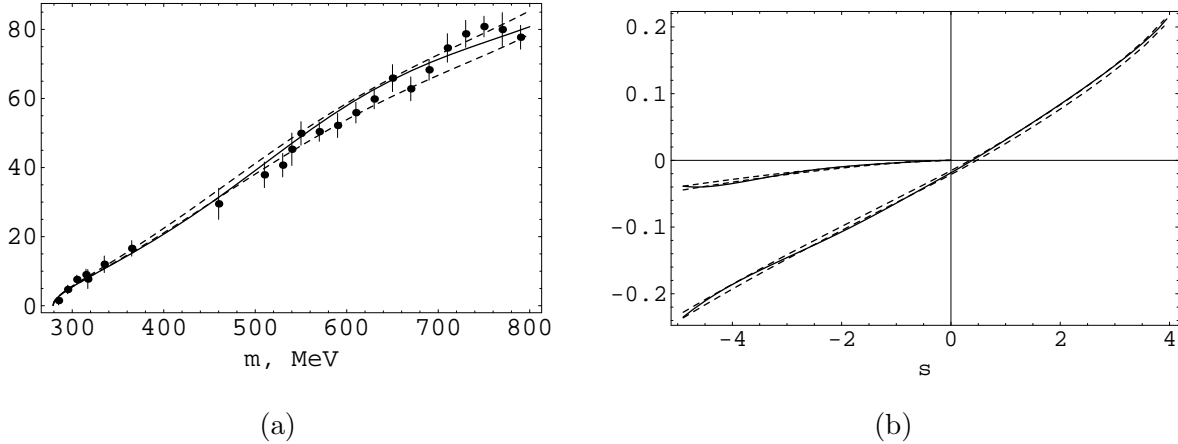


FIG. 13: a) The phase  $\delta_0^0$  of the  $\pi\pi$  scattering, Fit 3 is shown. The solid line is our description, dashed lines mark borders of the corridor [6], and points are experimental data. b) The real and the imaginary parts of the amplitude  $T_0^0$  of the  $\pi\pi$  scattering ( $s$  in units of  $m_\pi^2$ ) are shown. The solid lines correspond to Fit 3, dashed lines mark borders of the real part corridor and the imaginary part for  $s < 0$  [6].

requirement (30) and to improve the data description. The influence of this factor may be reduced in order to use a more skillful form than Eq. (31) for it.

New precise experimental data are needed for the investigation of light scalars. The elucidation of the situation, a contraction of the possible variants or even the selection of the unique variant, requires considerable effort. The new precise experiment on  $\pi\pi \rightarrow K\bar{K}$  would give the crucial information about the inelasticity  $\eta_0^0$  and about the phase  $\delta_B^{K\bar{K}}(m)$  near the  $K\bar{K}$  threshold. The forthcoming precise experiment in KLOE on the  $\phi \rightarrow \pi^0\pi^0\gamma$  decay will also help to judge this phase in an indirect way. The precise measurement of the inelasticity  $\eta_0^0$  near 1 GeV in  $\pi\pi \rightarrow \pi\pi$  would also be very important.

It is of interest to update our analysis of the  $\phi \rightarrow a_0(980)\gamma \rightarrow \eta\pi^0\gamma$  decay [23] and the  $\gamma\gamma \rightarrow a_0(980) \rightarrow \pi^0\eta$  description [43] in this analytical approach. Probably, such an approach would also be useful for the  $\kappa(900)$  meson investigation in the  $\pi K$  channel.

## VII. ACKNOWLEDGEMENTS

We thank very much H. Leutwyler for providing numerical values of the  $T_0^0(s)$  on the real axis, obtained in Ref. [6], useful discussions, and kind contacts. This work was supported

in part by RFBR, Grant No 10-02-00016.

- 
- [1] C. Amsler et al. (Particle Data Group), Phys. Lett. B **667**, 1 (2008).
  - [2] N.N. Achasov and A.V. Kiselev, Phys. Rev. **D73**, 054029 (2006); Erratum-ibid. **D74**, 059902 (2006); Yad. Fiz. **70**, 2005 (2007) [Phys. At. Nucl. **70**, 1956 (2007)].
  - [3] A.Aloisio et al. (KLOE Collaboration), Phys. Lett. **B537**, 21 (2002).
  - [4] N.N. Achasov and G.N. Shestakov, Phys. Rev. **D49**, 5779 (1994); Yad.Fiz. **56**, 206 (1993) [Phys. At. Nucl. **56**, 1270 (1993)]; Int. J. Mod. Phys. **A9**, 3669 (1994).
  - [5] N.N. Achasov and G.N. Shestakov, Phys. Rev. Lett. **99**, 072001 (2007).
  - [6] I. Caprini, G. Colangelo and H. Leutwyler, Phys. Rev. Lett. **96**, 132001 (2006).
  - [7] S.L. Adler, Phys. Rev. **B137**, 1022 (1965); ibid. **B139**, 1638 (1965).
  - [8] We met the opinion that the representation (2) violates analiticity, because the amplitude

$$T_{\pi\pi} = T_{res} + T_{back} + 2i\rho_{\pi\pi}T_{res}T_{back}$$

becomes infinite at  $s \rightarrow 0$  since  $\rho_{\pi\pi} \rightarrow \infty$  in this case ( $\rho_{\pi\pi} = \sqrt{1 - 4m_{\pi}^2/s}$ ). This obstacle may be overcome if  $T_{res}$  or  $T_{back}$  is equal to zero at  $s = 0$ . As in Ref. [2], we choose here the second variant,  $T_{back}(0) = 0$ .

- [9] N.N. Achasov and V.N. Ivanchenko, Nucl. Phys. **B315**, 465 (1989); Preprint INP 87-129 (1987) Novosibirsk.
- [10] N.N. Achasov and V.V. Gubin, Phys. Rev. **D56**, 4084 (1997); Yad. Fiz. **61**, 274 (1998) [Phys. At. Nucl. **61**, 224 (1998)].
- [11] N.N. Achasov, V.V. Gubin, Phys. Rev. **D63**, 094007 (2001); Yad. Fiz. **65**, 1566 (2002) [Phys. At. Nucl. **65**, 1528 (2002)].
- [12] N.N. Achasov and A.A. Kozhevnikov, Phys. Rev. **D61**, 054005 (2000); Yad. Fiz. **63**, 2029 (2000) [Phys. At. Nucl. **63**, 1936 (2000)].
- [13]  $F_b$  may be considerably less than 1 due to the  $\pi^0\pi^0$  final state interaction.
- [14] N.N. Achasov, S.A. Devyanin, and G.N. Shestakov, Phys. Lett. **96B**, 168 (1980).
- [15] N.N. Achasov, S.A. Devyanin, and G.N. Shestakov, Yad. Fiz. **32**, 1098 (1980)[Sov. J. Nucl. Phys. **32**, 566 (1980)].

- [16] N.N. Achasov, S.A. Devyanin and G.N. Shestakov, Z. Phys. **C22**, 53 (1984);
- [17] N.N. Achasov, S.A. Devyanin and G.N. Shestakov, Usp. Fiz. Nauk. **142**, 361 (1984) [Sov. Phys. Usp. **27**, 161 (1984)].
- [18] N.N. Achasov, S.A. Devyanin, and G.N. Shestakov, Phys. Lett. **88B**, 367 (1979).
- [19] N.N. Achasov and A.V. Kiselev, Phys. Rev. **D70**, 111901 (R) (2004).
- [20] N.N. Achasov, *THE SECOND DAΦNE PHYSICS HANDBOOK*, Vol. II, edited by L. Maiani, G. Panzeri, N. Paver, dei Laboratori Nazionali di Frascati, Frascati, Italy ( May 1995), p. 671.
- [21] N.N. Achasov and G.N. Shestakov, Usp. Fiz. Nauk. **161** (6), 53 (1991)[Sov. Phys. Usp. **34** (6), 471 (1991)]; N.N. Achasov, Nucl. Phys. B (Proc. Suppl.) **21**, 189 (1991); N.N. Achasov, Usp. Fiz. Nauk. **168**, 1257 (1998) [ Phys. Usp. **41**, 1149 (1998)]; N.N. Achasov, Nucl. Phys. **A675**, 279c (2000)
- [22] N.N. Achasov and V.V. Gubin, Phys. Rev. **D64**, 094016 (2001); Yad. Fiz. **65**, 1939 (2002) [Phys. At. Nucl. **65**, 1887 (2002)].
- [23] N.N. Achasov and A.V. Kiselev, Phys. Rev. **D68**, 014006 (2003); Yad. Fiz. **67**, 653 (2004) [Phys. At. Nucl. **67**, 633 (2004)].
- [24] M.N. Achasov et al, Phys. Rev. **D63**, 072002 (2001).
- [25] S.I. Dolinsky et al., Z. Phys. **C42**, 511 (1989).
- [26] M.N. Achasov et al, Phys. Lett. **B559**, 171 (2003).
- [27] Note that, in general, the existence of Adler zero in partial amplitudes is not obligatory, see APPENDIX II in Ref. [2].
- [28] Note that the condition (48) is similar to the condition (34) in PRD of Ref. [2] (in Phys. At. Nucl. it is (36)).
- [29] I. Caprini, Phys.Rev. **D 77**, 114019 (2008);  
G. Colangelo, J. Gasser and H. Leutwyler, Nucl. Phys. B 603 125 (2001).
- [30] R.L. Jaffe, Phys. Rev. **D15**, 267 (1977); **15**, 281 (1977).
- [31] B. Hyams et al., Nucl. Phys. **B64**, 134 (1973).
- [32] P. Estabrooks and A.D. Martin, Nucl. Phys. **B79**, 301 (1974).
- [33] A.D. Martin, E.N. Ozmutlu, E.J. Squires, Nucl. Phys. **B121**, 514 (1977).
- [34] V. Srinivasan et al., Phys. Rev. **D12**, 681 (1975).
- [35] L. Rosselet et al., Phys. Rev. **D15**, 574 (1977).

- [36] The same data was used in [2], but only up to 1.1 GeV. We add the data up to 1.2 GeV to provide better behaviour of our  $\delta_0^0$  and inelasticity, considering influence of high-energy resonances smaller than experimental errors.
- [37] S. Pislak et al., Phys. Rev. Lett. **87** 221801 (2001).
- [38] J.R. Batley et al., Eur. Phys. J. **C54**, 411 (2008).
- [39] A. Etkin et al, Phys. Rev. **D25**, 1786 (1982).
- [40] These constants are equal in the naive four-quark model.
- [41] In addition, propagators (8) are approximate, and their small difference with "real" propagators in the physical region could be important in the complex  $s$  plane.
- [42] D. Black, A. Fariborz, and J. Schechter, Phys. Rev. **D61** 074001 (2000).
- [43] N.N. Achasov and G.N. Shestakov, Phys. Rev. **D 81**, 094029 (2010).